Acta Physica Universitatis Comenianae
Vol. XLVI–XLVII, (2005–2006) 21–27

Numerical Simulation of Trochoidal Electron Monochromator

J. Matuška, D. Kubala, Š. Matejčík

Department of Experimental Physics, Comenius University, Bratislava, Mlynská dolina F2, 84248 Bratislava, Slovakia, March 6, 2006

Abstract: Trochoidal electron monochromator (TEM) using crossed homogenouse electric and magnetic fields has been investigated in a numerical simulation using the SIMION 7.0 package. The electron trajectory calculations have been carried out for a large number of initial electrons with finite energy spread and angular distribution function. The electron energy distribution function (EEDF) of the TEM has been studied as a function of the monochromator parameters. The numerical results have been compared with the experimental distribution functions.

1. Introduction

The beams of mono-energetic electrons are required in many experimental studies concerning electron interactions with the molecules in the gas phase or on the surfaces. The electron beams with well defined and narrow distribution functions (high energy resolution of the electron beams) can be formed with the help of electron monochromators.

There exist several types of the electron monochromators operation of which is based on different physical principles. To the most popular types belong the electrostatic monochromators (in cylindrical or spherical geometry) [1, 2] and the trochoidal electron monochromator (TEM)[3]. The TEM is able to produce the electron beams with currents in order of 10^{-9}nA and the electron energy resolution down to 20 meV. At low electron energies, the effect of electrostatic repulsion of the electrons may play a significant role in the electrostatic monochromators. This problem can be omitted if axial magnetic field is applied, however, the presence of the magnetic fields is harmful for the operation of the electrostatic monochromators. On the other hand, the trochoidal electron monochromator is based on the dispersive properties of the perpendicular homogeneous electric and magnetic fields. The magnetic field is axially aligned with the axis of the monochromator. For this reason the TEM is popular in applications where low energy electron beams are required [4 9].

In present paper, we discuss the basic attributes of the TEM operation on the basis of numerical simulation of the TEM. Using the SIMION [10] charge particle optics program, detailed three dimensional numerical calculations of the electrostatic fields in the TEM have been performed. The principle of operation of the TEM has been investigated earlier [11 13]. These analytical studies were performed only for the simplified case neglecting transversal velocities of the electrons, fringing field. Grill et al. [14] carried out three dimensional study of the TEM, however, only in a very limited range of electron energies

and angles. In present work, we have performed numerical simulation of the transmission of the electrons through the monochromator. The electric fields were calculated for real geometry of the electrodes. Thus, the calculated electric fields includes the fringing fields at apertures of the electrodes. The trajectories have been calculated for a large number of the electrons in different initial state (kinetic energy and the direction) simulating the thermionic emission of the electrons from the filament.

The geometry of the simulated TEM was identical with the TEM used in our laboratory [15]. The aim of this study was to simulate the operation of the TEM and to estimate, on the basis of the simulation, the electron energy distribution function (EEDF) of the electron beam formed in the monochromator and to compare it with the experimental one. It is also assumed [17] that the EEDF may depend on the energy of the electrons, however, there exists, so far, no systematic study of this effect. In the present work we have simulated the EEDF in the electron energy range from 0 to 100 eV and observed broadening of the EEDF.

2. Principles of the Operation

The dispersive element of the TEM is showed in Fig. 1. The separation of the electrons occurs in a space with crossed perpendicular homogeneous electrostatic $\vec{E}$ and magnetic fields $\vec{B}$. The electric field produced by a pair of parallel plain electrodes (length L in the axial direction) has only the y component. The magnetic field formed by the Helmholz coils has only the x component and is axially aligned with the original direction of the electrons. The velocity $\vec{v}_0$ of the electrons entering the dispersive element is parallel to the magnetic field and has the x direction. The Lorentzian force acts on the electron. The trajectory of the electrons in such fields can be obtained as a solution of the differential equation:

$$m_e \frac{d^2\vec{r}}{dt^2} \quad e\vec{E} \quad e\vec{v} \quad \vec{B} \tag{1}$$

where $\vec{B} = (B, 0, 0)$, $\vec{E} = (0,E, 0)$ and $\vec{v}_0 = (v_0, 0, 0)$. This equation can be expanded in the system of differential equations.

$$m_e \frac{d^2x}{dt} \quad ev_y B \tag{2}$$

$$m_e \frac{d^2y}{dt} \quad eE \quad ev_x B \tag{3}$$

$$m_e \frac{d^2z}{dt} \quad 0 \tag{4}$$

There exists analytical solution for this system of equations [3, 14]. In the z direction a constant drift velocity $\vec{v}_D$ exists, which depends only on the magnitude of the electric and magnetic fields and is velocity independent:

$$\vec{v}_D \quad \frac{\vec{E} \quad \vec{B}}{B^2} \tag{5}$$

The drift velocity can be used to separate electrons according to the magnitude of the x component of the initial velocity. The fast electrons spend relatively short time in the

dispersive element and thus, at the end of the element, only small deflection in z direction is observed. On the other hand the slow electrons spend a longer time in the dispersive element and, thus, their deflection in z direction is larger. The apertures at the beginning and at the end of the crossed field space have different z coordinates. Thus, only electrons with proper initial velocity and with narrow energy spread may leave the dispersive space. More details on the analytical theory of the TEM are given in papers [3, 14].

This analytical model illustrates only the basic attributes of TEM monochromator and cannot describe all properties like the influence of the inhomogenities in the electric fields, the trajectories of the electrons with different initial angular orientation and the initial energy distribution function of the electrons in the TEM. In order to get better understanding of the TEM operation, we have decided to perform numerical trajectory simulation of TEM.

3. Numerical Simulation

The numerical simulation of the TEM has been performed using the charge particle optics program SIMION 3D 7.0 [10]. This software is a powerful instrument for numerical calculations of the electrostatic fields for a system of electrodes. Moreover, this software is able to calculate the ion and electron trajectories in the system of electrostatic and magnetic fields.

The simulated TEM has the geometry and the dimensions of the TEM built at the Department of Experimental Physics, Comenius University [16]. The detailed design including reaction chamber is shown in Fig. 2. The electrodes made from stainless steel are 1.2 mm thick and the distances between the electrodes are 1.0 mm. The apertures of the electrodes in the model are cylindrical in contrast to the funnel shape of the apertures in the real monochromator. The funnel shape apertures are used in order to decrease the charging of the apertures due to adsorption of the molecules on the apertures. We neglect this effect in the present model. The diameter of the apertures is 1.0 mm. The dispersive element of TEM is 20 mm long. The entrance aperture of the dispersive element is 2 mm of axis. The exit aperture is exactly in the center of the electrode (Fig. 1).

The EEDF of the electron beam formed in the TEM is determined i) by the initial distribution function of electrons emitted from filament and ii) by the dispersive properties of the electron monochromator. The electron source of the real TEM is a hairpin filament directly heated by passing electric current. The electrons are emitted from the tip of the filament by thermionic emission. In present simulation we have approximated the filament by a point and we assume that the initial distribution functions of the electrons is determined by the thermionic emission. Thus the initial EEDF has thus an exponential character.

$$f(E) \quad \exp \quad \frac{E}{kT} \tag{6}$$

where $f(E)$ is the relative abundance of the electrons with kinetic energy E, T is the temperature of metal. In this simulations, we have not considered the mutual repulsion (Coulomb repulsion) of the electrons. We neglect this effect due to the fact that we have been using magnetic field in axial direction, which prevents the repulsion.

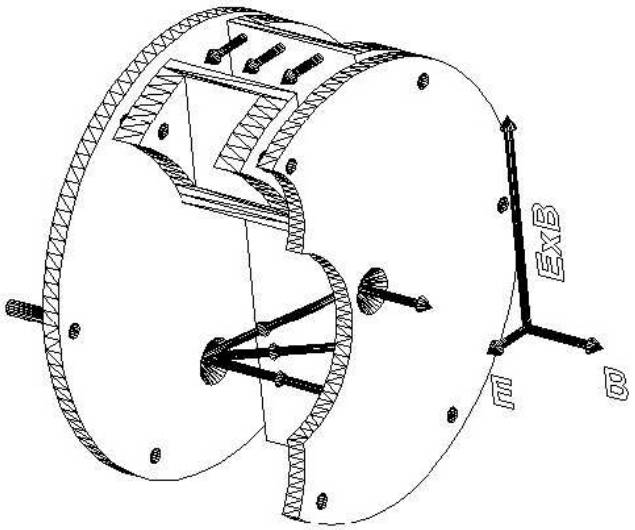

Fig. 1. The dispersive element of the TEM monochromator.

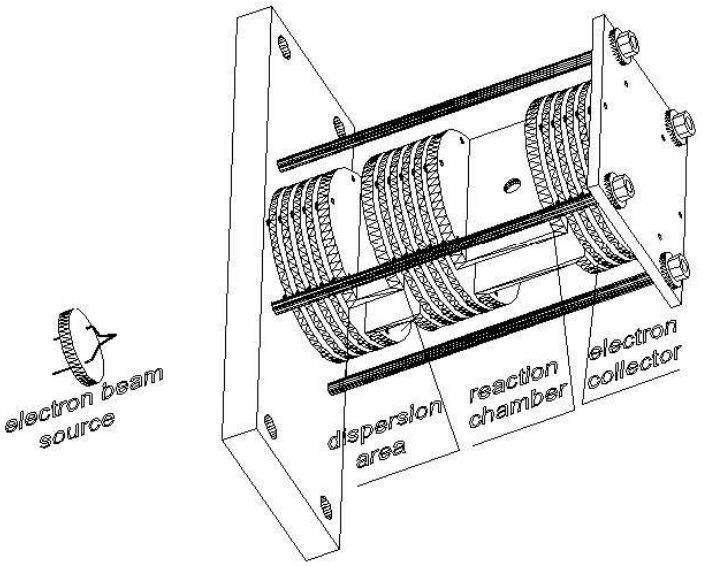

Fig. 2. The picture of the simulated trochoidal electron monochromator.

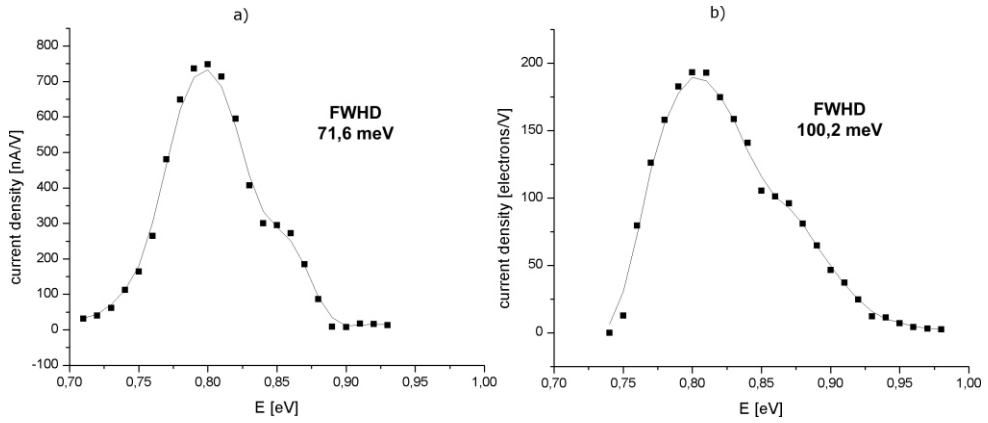

Fig. 3. Comparison of the EEDF of the electrons obtained in a) experiment and b) simulation.

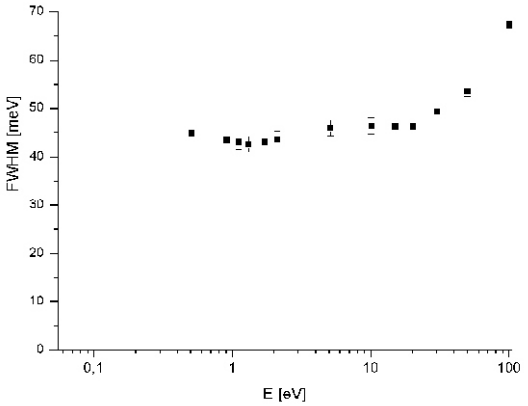

Fig. 4. The dependence of the width of the EEDF on the energy of the electrons. Note that this set of data has been calculated under different monochromator parameters then the previouse data.

4. Results and Discussion

In the present work we have performed trajectory calculations of the electrons trough the TEM. The trajectory calculations have been carried out with a large number of electrons (appr. 10 000) with different initial parameters (electron energy and direction). The initial EEDF was given by the thermionic emission of the electrons from the cathode. The number of the electrons, which hit the last electrode (Faraday cup), and their energy have been recorded and evaluated. A histogram obtained in this way correspond to the EEDF of the TEM. The calculated EEDF is presented in Fig. 3a. The simulated EEDF have been

compared with the EEDF of the electron beams of the real monochromator. The EEDFs of the real monochromator have been measured using the retarding potential field method [?]. The potentials of the particular electrodes and also the intensity of the magnetic field in the simulation have been set to the values used in the experiment.

The results for one particular set of electrode potentials (identical settings were applied in the experiment and in the simulation) are shown in Fig. 3. On the right site the EEDF obtained in the numerical simulation is presented, whereas on the left site the experimental one is shown. The shapes of these two EEDF are remarkably similar. Beside the main peaks there are two shoulders present at the high energy site of the EEDF. There nature of these shoulders will be the object of our future studies. There exists difference in the width of the EEDF at half maximum (full width at half maximum - FWHM). The calculated FWHM of approximatelly 100 meV overestimated the FWHM of the experimental EEDF of 72 meV. Similar calculations have been carried out for further sets of the electrode potentials and different electron energies.

The retarding potential difference method may be applied in the experiment to measure EEDF only at low electron energies. At high electron energies, there exist problems due to such effects as the secondary electron emission of the electrons and reflection of the electrons from the Faraday cup. However, we have applied the simulation in order to account for the effect of the electron energy on the EEDF. In this simulation all potential of the TEM have been kept constant with one exception - we have varied the acceleration potential in the interval from 0 up to 100 V. The results of the calculations are showed in Fig. 3. In the energy interval from 0 to 15 eV the width of the EEDF was practically constant. This result is particularly interesting, as in this electron energy range, the dissociative electron attachment reactions are measured. In earlier dissociative electron attachment studies [17] it was believed that already in this electron energy range strong variations of the EEDF occur. Only weak fluctuations have been observed but they are comparable with the uncertainty of the measured values. Above 15 eV, the width of the EEDF slowly increases. However, the increase is not as dramatical as expected. At electron energy of 100 eV the width of the EEDF is about 60 % larger then at low electron energies.

5. Conclusions

Using the numerical simulation, we have calculated the EEDF of the electrons in the electron beam formed in the TEM. We have obtained agreement between the shapes of the calculated and experimental EEDF. Additionally, the dependence of the EEDF on the acceleration potential has been calculated. The width of the EEDF between 1 and 100 eV increased by about 60 %.

Acknowledgment

This work was supported by Science and Technology Assistance Agency under contract No. APVT-20-007504.

References

[1] D. Roy, P. D. Burrow: J. Phys. E **8** (1975) 273.
[2] K. Jost: J. Phys. E **12** (1979) 1006.
[3] A. Stamatovic, G. J. Schulz: Rev. Sci. Instrum. **41** (1970) 423.
[4] A. R. Johnston, P. D. Burrow: J. Phys. B: At. Mol. Phys. **16** (1983) 613.
[5] P. Cloutier, L. Sanche: Rev. Sci. Instrum. **60** (1989) 1054.
[6] M. Zubek: J. Phys. B: At. Mol. Opt. Phys. **27** (1994) 573 581.
[7] M. Allan: Helv. Chim. Acta **65** (1982) 2008.
[8] E. Illenberger: Chem. Rev. **92** (1992) 1589.
[9] S. Matejcik, G. Senn, P. Scheier, A. Kiendler, A. Stamatovic, T. D. Mark: J. Chem. Phys. **107** (1997) 8955 8962.
[10] NIST, SIMION, program.
[11] D. Roy: Rev. Sci. Instrum. **43** (1972) 535.
[12] M. I. Romanyuk, O. B. Shpenik: Meas. Sci. Technol. **5** (1994) 239.
[13] I. D. Williams, R. W. O'Neill: Meas. Sci. Technol. **6** (1995) 1133.
[14] V. Grill, H. Drexel, W. Sailer, M. Lezius, T. D. Mark: Int. J. Mass Spect. **205** (2001) 209.
[15] S. Matejcik, V. Foltin, M. Stano, J. D. Skalny: Int. J. Mass Spect. **9** (2003) 223 224.
[16] M. Stano, S. Matejcik, J. D. Skalny, T. D. Markk: J. Phys. B: At. Mol. Opt. Phys. **36** (2003) 261.
[17] Y. Chu, G. Senn, S. Matejcik: Chem. Phys. Letters **289** (1998) 521.